IUAC School on Nuclear Reactions: The CDCC and CRC methods

Antonio M. Moro

Universidad de Sevilla, Spain

November 15th-20th, 2021

Material available at: `https://github.com/ammoro/IUAC`

Course outline I

1. The CDCC method
   - Reminder of the coupled-channels method
   - Single-particle and cluster excitations
   - Partial wave analysis: radial equations
   - Some examples of applications of the CDCC method
   - Exploring the continuum with breakup reactions
   - Radiative capture from Coulomb dissociation data
2. Advanced CDCC and extensions
   - Extension to 3-body projectiles
   - Core excitations

Motivation of the CDCC method

How does the halo structure affect the elastic scattering?

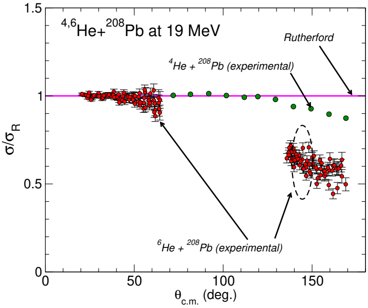

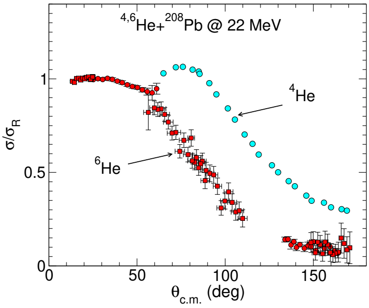

- For $E = 19$ MeV (below the barrier, $V_b \approx 21$ MeV) ^{4}He follows Rutherford formula.
- ^{6}He drastically departs from Rutherford formula at both energies!

Motivation of the CDCC method

How does the halo structure affect the elastic scattering?

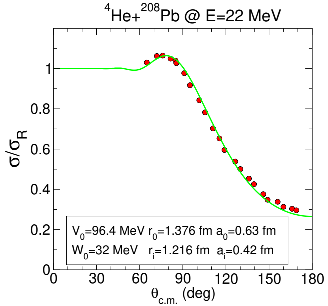

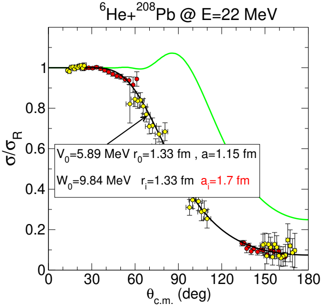

- ➩ ^{4}He+^{208}Pb shows typical Fresnel pattern and “standard” optical model parameters
- ➩ ^{6}He+^{208}Pb shows a prominent reduction in the elastic cross section, suggesting that part of the incident flux goes to nonelastic channels (e.g. breakup, transfer...)
- ☞ Understanding and disentangling these nonelastic channels requires going beyond the optical model (eg. coupled-channels method)

Reminder of the coupled-channels method

Inelastic scattering

- Nuclei are not inert or *frozen* objects; they do have an internal structure of protons and neutrons that can be modified (excited) during the collision.
- Quantum systems exhibit, in general, an energy spectrum with bound and unbound levels.

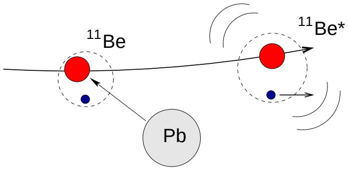

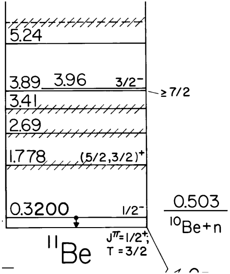

Models for inelastic excitations

1. COLLECTIVE: Involve a collective motion of several nucleons which can be interpreted macroscopically as rotations or surface vibrations of the nucleus.

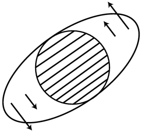

2. FEW-BODY/SINGLE-PARTICLE: Involve the excitation of a nucleon or cluster.

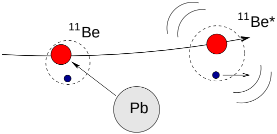

The coupled-channels method for inelastic scattering

We need to incorporate explicitly in the Hamiltonian the internal structure of the nucleus being excited (e.g. projectile).

$$\boxed{H = T_R + h(\xi) + V(\mathbf{R}, \xi)}$$

- T_R: Kinetic energy for projectile-target relative motion.
- $\{\xi\}$: Internal degrees of freedom of the projectile (depend on the model).
- $V(\mathbf{R}, \xi)$: Projectile-target interaction.
- $h(\xi)$: Internal Hamiltonian of the projectile.

$$\boxed{h(\xi)\phi_n(\xi) = \varepsilon_n \phi_n(\xi)}$$

- $\phi_n(\xi)$: internal states of the projectile.

Modelscape and scattering wavefunction: d+^{10}Be → d+^{10}Be* example

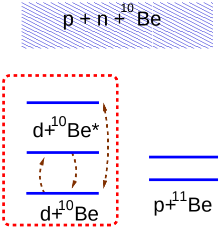

☞ The modelspace is composed by ground states (elastic channel) and some excited states (inelastic scattering)

Boundary conditions for scattering wavefunction:

$$\Psi^{(+)}_{\mathbf{K}_0}(\mathbf{R},\xi) \xrightarrow{R\gg} \underbrace{e^{i\mathbf{K}_0\cdot\mathbf{R}}\phi_0(\xi)}_{\text{incident}} + \underbrace{f_{0,0}(\theta)\frac{e^{iK_0R}}{R}\phi_0(\xi)}_{\text{elastic}} + \underbrace{\sum_{n>0} f_{n,0}(\theta)\frac{e^{iK_nR}}{R}\phi_n(\xi)}_{\text{inelastic}}$$

Cross sections:

$$\left(\frac{d\sigma(\theta)}{d\Omega}\right)_{0\to n} = \frac{K_n}{K_0}|f_{n,0}(\theta)|^2 \qquad f_{n,0}(\theta) = \text{scattering amplitude}$$

CC model wavefunction (target excitation)

We expand the total wave function in a subset of internal states representing the adopted modelspace:

$$\boxed{\Psi_{\rm model}(\mathbf{R},\xi) = \phi_0(\xi)\chi_0(\mathbf{K}_0,\mathbf{R}) + \sum_{n>0}\phi_n(\xi)\chi_n(\mathbf{K}_n,\mathbf{R})}$$

and impose the boundary conditions for the (unknown) $\chi_n(\mathbf{R})$:

$$\chi_0^{(+)}(\mathbf{K}_0,\mathbf{R}) \to e^{i\mathbf{K}_0\cdot\mathbf{R}} + f_{0,0}(\theta)\frac{e^{iK_0R}}{R} \qquad \text{for n=0 (elastic)}$$

$$\chi_n^{(+)}(\mathbf{K}_n,\mathbf{R}) \to f_{n,0}(\theta)\frac{e^{iK_nR}}{R} \qquad \text{for n>0 (non-elastic)}$$

Calculation of $\chi_n^{(+)}(\mathbf{R})$: the coupled equations

- The model wavefunction must satisfy the Schrödinger equation:

$$[H - E]\Psi^{(+)}_{\text{model}}(\mathbf{R}, \xi) = 0$$

- Multiply on the left by each $\phi_n^*(\xi)$, and integrate over $\xi \Rightarrow$ coupled channels equations for $\{\chi_n(\mathbf{R})\}$:

$$\boxed{[E - \varepsilon_n - T_R - V_{n,n}(\mathbf{R})]\chi_n(\mathbf{R}) = \sum_{n' \neq n} V_{n,n'}(\mathbf{R})\chi_{n'}(\mathbf{R})}$$

- The structure information is embedded in the coupling potentials:

$$\boxed{V_{n,n'}(\mathbf{R}) = \int d\xi \phi^*_{n'}(\xi) V(\mathbf{R}, \xi)\phi_n(\xi)}$$

☞ *$\phi_n(\xi)$ will depend on the assumed structure model (collective, few-body, etc).*

Optical Model vs. Coupled-Channels method

Optical Model

- The Hamiltonian:
  $H = T_R + V(\mathbf{R})$
- Internal states: Just $\phi_0(\xi)$
- Model wavefunction:
  $\Psi_{\rm mod}(\mathbf{R}, \xi) \equiv \chi_0(\mathbf{K}, \mathbf{R})\phi_0(\xi)$
- Schrödinger equation:
  $[H - E]\chi_0(\mathbf{K}, \mathbf{R}) = 0$

Optical Model vs. Coupled-Channels method

Optical Model

- The Hamiltonian:
  $H = T_R + V(\mathbf{R})$
- Internal states: Just $\phi_0(\xi)$
- Model wavefunction:
  $\Psi_{\rm mod}(\mathbf{R},\xi) \equiv \chi_0(\mathbf{K},\mathbf{R})\phi_0(\xi)$
- Schrödinger equation:
  $[H-E]\chi_0(\mathbf{K},\mathbf{R}) = 0$

Coupled-channels method

- The Hamiltonian:
  $H = T_R + h(\xi) + V(\mathbf{R},\xi)$
- Internal states:
  $h(\xi)\phi_n(\xi) = \varepsilon_n\phi_n(\xi)$
- Model wavefunction:
  $\Psi_{\rm model}(\mathbf{R},\xi) = \phi_0(\xi)\chi_0(\mathbf{K},\mathbf{R}) + \sum_{n>0}\phi_n(\xi)\chi_n(\mathbf{K},\mathbf{R})$
- Schrödinger equation:

$$[H-E]\Psi_{\rm model}(\mathbf{R},\xi) = 0$$

$$\Downarrow$$

$$[E-\varepsilon_n - T_R - V_{n,n}(\mathbf{R})]\chi_n(\mathbf{K},\mathbf{R}) = \sum_{n'\neq n} V_{n,n'}(\mathbf{R})\chi_{n'}(\mathbf{K},\mathbf{R})$$

DWBA approximation as 1st order CC

- Two-states model $n = 0, 1$:

$$\Psi(\mathbf{R}, \xi) = \underbrace{\phi_0(\xi)\chi_0(\mathbf{R})}_{\text{elastic}} + \underbrace{\phi_1(\xi)\chi_1(\mathbf{R})}_{\text{inelastic}}$$

- Coupled-channels equations:

$$[E - \varepsilon_0 - T_0 - V_{00}(\mathbf{R})]\,\chi_0(\mathbf{R}) = V_{01}(\mathbf{R})\chi_1(\mathbf{R})$$
$$[E - \varepsilon_1 - T_1 - V_{11}(\mathbf{R})]\,\chi_1(\mathbf{R}) = V_{10}(\mathbf{R})\chi_0(\mathbf{R})$$

- Iterative solution of the CC equations (DWBA):

$$[E - \varepsilon_0 - T_0 - V_{00}(\mathbf{R})]\,\chi_0(\mathbf{R}) \approx 0$$
$$[E - \varepsilon_1 - T_1 - V_{11}(\mathbf{R})]\,\chi_1(\mathbf{R}) \approx V_{10}(\mathbf{R})\chi_0(\mathbf{R})$$

DWBA approximation as 1st order CC

- Asymptotically:

$$\chi_1^{(+)}(\mathbf{R}) \to f_{10}(\theta)\frac{e^{iK_1 R}}{R}$$

with (not proven here!)

$$\boxed{f_{10}(\theta) = -\frac{2\mu}{4\pi\hbar^2}\int d\mathbf{R}\widetilde{\chi}_1^{(-)*}(\mathbf{K}_1,\mathbf{R})V_{10}(\mathbf{R})\widetilde{\chi}_0^{(+)}(\mathbf{K}_0,\mathbf{R})}$$

where $\widetilde{\chi}_0(\mathbf{K}_0,\mathbf{R})$, $\widetilde{\chi}_1(\mathbf{K}_1,\mathbf{R})$ are solutions of:

$$[E-\varepsilon_0-T_0-V_{00}(\mathbf{R})]\widetilde{\chi}_0(\mathbf{K}_0,\mathbf{R}) = 0$$
$$[E-\varepsilon_1-T_1-V_{11}(\mathbf{R})]\widetilde{\chi}_1(\mathbf{K}_1,\mathbf{R}) = 0$$

☞ *The DWBA approximation amounts at solving the CC equations to 1st order (Born approximation)*

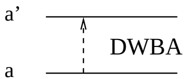

Single-particle and cluster excitations

Many-body to few-body reduction

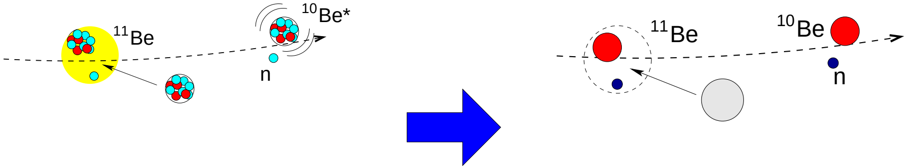

$$\mathcal{V}_{pt} = \sum_{ij} V_{ij}(\mathbf{r}_{ij})$$

$$\mathcal{V}_{pt} = U_{ct}(\mathbf{r}_{ct}) + U_{nt}(\mathbf{r}_{nt})$$

- Effective three-body Hamiltonian:

$$\boxed{H = T_{\mathbf{R}} + h_r(\mathbf{r}) + U_{ct}(\mathbf{r}_{ct}) + U_{nt}(\mathbf{r}_{nt})}$$

- $U_{ct}(\mathbf{r}_{ct})$, $U_{nt}(\mathbf{r}_{nt})$ are optical potentials describing fragment-target elastic scattering (eg. target excitation is treated effectively, through absorption)

Inelastic scattering in a few-body model

- Some nuclei allow a description in terms of two or more clusters: d=p+n, ^{6}Li=α+d, ^{7}Li=α+^{3}H.
- Projectile-target interaction:

$$V(\mathbf{R},\xi) \equiv V(\mathbf{R},\mathbf{r}) = U_1(\mathbf{r}_1) + U_2(\mathbf{r}_2)$$

- Transition potentials:

$$\boxed{V_{n,n'}(\mathbf{R}) = \int d\mathbf{r}\phi^*_n(\mathbf{r})\,[U_1(\mathbf{r}_1) + U_2(\mathbf{r}_2)]\,\phi_{n'}(\mathbf{r})}$$

Inelastic scattering in a few-body model

- Some nuclei allow a description in terms of two or more clusters: d=p+n, ^{6}Li=α+d, ^{7}Li=α+^{3}H.
- Projectile-target interaction:

$$V(\mathbf{R},\xi) \equiv V(\mathbf{R},\mathbf{r}) = U_1(\mathbf{r}_1) + U_2(\mathbf{r}_2)$$

- Transition potentials:

$$\boxed{V_{n,n'}(\mathbf{R}) = \int d\mathbf{r}\phi^*_n(\mathbf{r})\,[U_1(\mathbf{r}_1) + U_2(\mathbf{r}_2)]\,\phi_{n'}(\mathbf{r})}$$

Example: ^{7}Li=α+t

$$\mathbf{r}_\alpha = \mathbf{R} - \frac{m_t}{m_\alpha + m_t}\mathbf{r}; \quad \mathbf{r}_t = \mathbf{R} + \frac{m_\alpha}{m_\alpha + m_t}\mathbf{r}$$

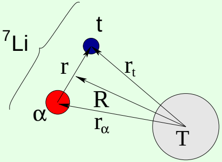

Internal states: (two-body cluster model)

$$[T_{\mathbf{r}} + V_{\alpha-t}(\mathbf{r}) - \varepsilon_n]\phi_n(\mathbf{r}) = 0$$

Example: ^{7}Li(α+t) +^{208}Pb at 68 MeV

➩ CC calculation with 2 channels ($3/2^-$, $1/2^-$):

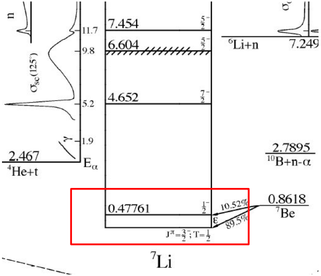

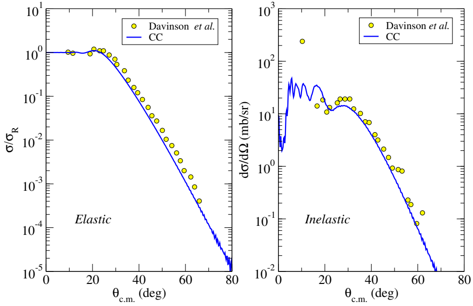

Data from Davinson et al, Phys. Lett. 139B (1984) 150)

☞ Fresco input available at `https://github.com/ammoro/IUAC`

Application of the CC method to weakly-bound systems

Example: Three-body calculation (p+n+^{58}Ni) with Watanabe potential:

$$V_{dt}(\mathbf{R}) = \int d\mathbf{r}\phi^*_{\rm gs}(\mathbf{r})\left\{V_{pt}(\mathbf{r}_{pt}) + V_{nt}(\mathbf{r}_{nt})\right\}\phi_{\rm gs}(\mathbf{r})$$

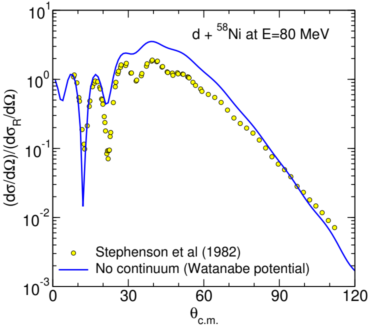

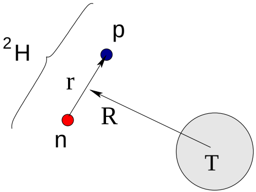

☞*Three-body calculations omitting breakup channels fail to describe the experimental data.*

Extension of the CC to unbound states

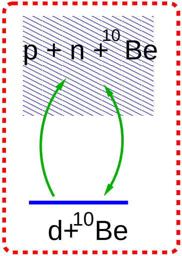

☞*We want to include explicitly in the modelspace the breakup channels of the projectile or target.*

Bound versus scattering states

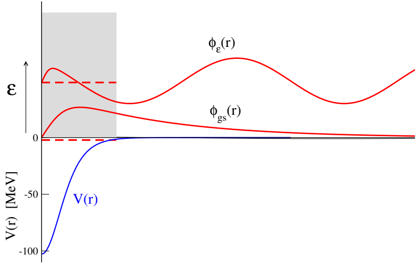

Continuum wavefunctions:

$$\varphi_{k,\ell jm}(\mathbf{r}) = \frac{u_{k,\ell j}(r)}{r}[Y_\ell(\hat{r}) \otimes \chi_s]_{jm}$$

$$\varepsilon = \frac{\hbar^2 k^2}{2\mu}$$

Bound versus scattering states

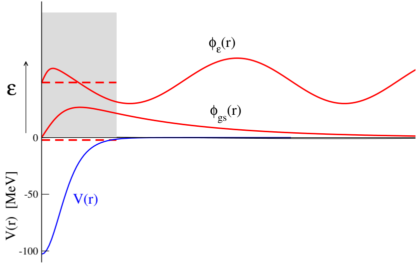

Continuum wavefunctions:

$$\varphi_{k,\ell jm}(\mathbf{r}) = \frac{u_{k,\ell j}(r)}{r}[Y_\ell(\hat{r}) \otimes \chi_s]_{jm}$$

$$\varepsilon = \frac{\hbar^2 k^2}{2\mu}$$

Unbound states are not suitable for CC calculations:

- They have a continuous (infinite) distribution in energy.
- Non-normalizable: $\langle u_{k,\ell sj}(r) | u_{k',\ell sj}(r) \rangle \propto \delta(k - k')$

SOLUTION ⇒ continuum discretization

The origins of CDCC

- Continuum discretization method proposed by G.H. Rawitscher [PRC9, 2210 (1974)] and Farrell, Vincent and Austern [Ann.Phys.(New York) 96, 333 (1976)] to describe deuteron scattering as an effective three-body problem $p + n + A$.

PHYSICAL REVIEW C VOLUME 9, NUMBER 6 JUNE 1974

Effect of deuteron breakup on elastic deuteron-nucleus scattering

George H. Rawitscher*
Center for Theoretical Physics, Massachusetts Institute of Technology, Cambridge, Massachusetts 02139,†
and Department of Physics, University of Surrey, Guildford, Surrey, England
(Received 1 October 1973; revised manuscript received 4 March 1974)

The properties of the transition matrix elements $V_{ab}(R)$ of the breakup potential V_N taken between states $\phi_a(\vec{r})$ and $\phi_b(r)$ are examined. Here $\phi_a(\vec{r})$ are eigenstates of the neutron-proton relative-motion Hamiltonian, and the eigenvalues of the energy ϵ_a are positive (continuum states) or negative (bound deuteron); $V_N(\vec{r}, \vec{R})$ is the sum of the phenomenological proton nucleus $V_{p-A}(|\vec{R}-\frac{1}{2}\vec{r}|)$ and neutron nucleus $V_{n-A}(|\vec{R}+\frac{1}{2}\vec{r}|)$ optical potentials evaluated for nucleon energies equal to half the incident deuteron energy. The bound-to-continuum transition matrix element for relative neutron-proton angular momenta $l=2$ are found to be comparable in magnitude to the ones for $l=0$ for values of ϵ_a larger than about 3 MeV, and both decrease only slowly with ϵ_a, suggesting that a large breakup spectrum is involved in deuteron-nucleus collisions. The effect of the various breakup transitions on the elastic phase shifts is estimated by numerically solving a set of coupled equations. These equations couple the functions $\chi_a(\vec{R})$ which are the coefficients of the expansion of the neutron-proton-nucleus wave function in a set of the $\phi_a(\vec{r})$'s. The equations are rendered manageable by performing a (rather crude) discretization in the neutron-proton relative-momentum variable k_a. Numer-

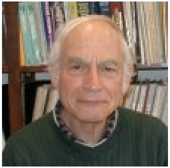

George Rawitscher (1928-2018)

- Full numerical implementation by Kyushu group (Sakuragi, Yahiro, Kamimura, and co.): Prog. Theor. Phys.(Kyoto) 68, 322 (1982)

Continuum discretization for deuteron scattering

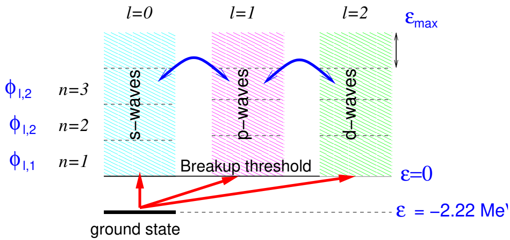

- Select a number of angular momenta ($\ell = 0, \ldots, \ell_{\max}$).
- For each ℓ, set a maximum excitation energy $\varepsilon_{\max}$.
- Divide the interval $\varepsilon = 0 - \varepsilon_{\max}$ in a set of sub-intervals (*bins*).
- For each bin, calculate a representative wavefunction.

CDCC formalism: construction of the bin wavefunctions

Bin wavefunction:

$$\phi_{\ell jm}^{[k_1,k_2]}(\mathbf{r}) = \frac{u_{\ell j}^{[k_1,k_2]}(r)}{r}[Y_\ell(\hat{r}) \otimes \chi_s]_{jm} \qquad [k_1, k_2] = \text{bin interval}$$

$$\boxed{u_{\ell sjm}^{[k_1,k_2]}(r) = \sqrt{\frac{2}{\pi N}} \int_{k_1}^{k_2} w(k) u_{k,\ell sj}(r) dk}$$

- k: linear momentum
- $u_{k,\ell sj}(r)$: scattering states (radial part)
- $w(k)$: weight function

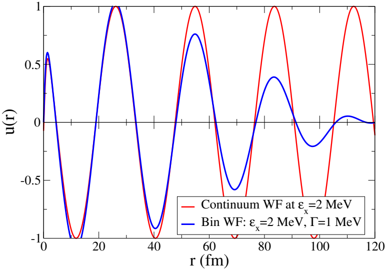

CDCC formalism for deuteron scattering

- Hamiltonian: $H = T_{\mathbf{R}} + h_r(\mathbf{r}) + V_{pt}(\mathbf{r}_{pt}) + V_{nt}(\mathbf{r}_{nt})$
- Model wavefunction:

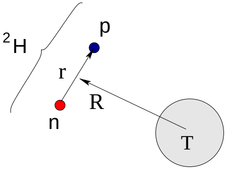

$$\Psi^{(+)}(\mathbf{R},\mathbf{r}) = \phi_{gs}(\mathbf{r})\chi_0(\mathbf{R}) + \sum_{n>0}^{N} \phi_n(\mathbf{r})\chi_n(\mathbf{R})$$

  - Coupled equations: $[H - E]\Psi(\mathbf{R},\mathbf{r}) = 0$

$$\boxed{[E - \varepsilon_n - T_R - V_{n,n}(\mathbf{R})]\chi_n(\mathbf{R}) = \sum_{n' \neq n} V_{n,n'}(\mathbf{R})\chi_{n'}(\mathbf{R})}$$

  - Transition potentials:

$$V_{n;n'}(\mathbf{R}) = \int d\mathbf{r}\phi_n^*(\mathbf{r})\left[V_{pt}(\mathbf{R} + \frac{\mathbf{r}}{2}) + V_{nt}(\mathbf{R} - \frac{\mathbf{r}}{2})\right]\phi_{n'}(\mathbf{r})$$

Partial-wave decomposition of CDCC wavefunction

- In practical calculations, the CDCC wf is expanded in the so-called channel basis $\langle \hat{R}, \mathbf{r}, |\beta; J_T\rangle = \left[Y_L(\hat{R}) \otimes \phi_{n,J_p}(\mathbf{r}) \right]_{J_T}$:

$$\boxed{\Psi_{\beta_0,J_T,M_T}(\vec{R}, \vec{r}, \xi) = \sum_{\beta} \frac{\chi^{J_T}_{\beta,\beta_0}(R)}{R} |\beta; J_T\rangle \quad \beta \equiv \{L, J_p, n\}}$$

- The radial coefficients verify

$$\boxed{\left(-\frac{\hbar^2}{2\mu}\frac{d^2}{dR^2} + \frac{\hbar^2 L(L+1)}{2\mu R^2} + \varepsilon_n - E \right) \chi^{J_T}_{\beta,\beta_0}(R) + \sum_{\beta} V^{J_T}_{\beta,\beta'}(R)\chi^{J_T}_{\beta'}(R) = 0}$$

with the coupling potentials:

$$\boxed{V^{J_T}_{\beta,\beta'}(R) = \langle \beta; J_T | V_1(\vec{R}, \vec{r}) + V_2(\vec{R}, \vec{r}) | \beta'; J_T \rangle}$$

- Boundary conditions:

$$\boxed{\chi^{J_T}_{\beta,\beta_0}(R) \to e^{i\sigma_L} \frac{i}{2} \left[H^{(-)}_L(K_\beta R)\delta_{\beta_0,\beta} - S^{J_T}_{\beta,\beta_0} H^{(+)}_L(K_\beta R) \right]}$$

Applications of the CDCC formalism: d+ ^{58}Ni

Coupling to continuum states produce:

- Polarization of the projectile (modification of real part)
- Flux removal (absorption) from the elastic channel (imaginary part)

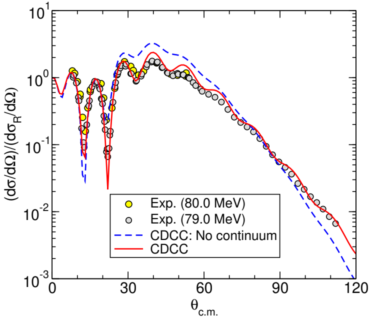

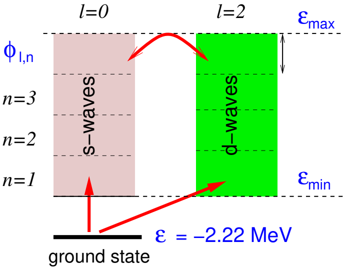

Two- and three-body breakup observables

- CDCC scattering amplitudes readily provide **two-body breakup** observables:

$$\boxed{\frac{d\sigma_n}{d\Omega_{\text{c.m.}}} = |f_{0,n}(\theta)|^2 \Rightarrow \frac{d^2\sigma}{d\Omega_{\text{c.m.}} d\epsilon_{pn}} \simeq \frac{1}{\Delta_n} \frac{d\sigma_n}{d\Omega_{\text{c.m.}}}}$$

with:

- Δ_n=width of the bin containing the relative energy ϵ_{pn}
- $\Omega_{\text{c.m.}}$=C.M. scattering angle of the projectile c.m. (not easy to measure!)

- **Three-body observables** can be also calculated using a suitable combination of the scattering amplitudes and appropriate kinematical transformations (Tostevin, PRC63, 024617 (2001)):

$$\boxed{\frac{d^3\sigma}{d\Omega_n d\Omega_p dE_p}}$$

☞ **N.b.:** *These 3-body observables are not directly provided by FRESCO. They must be computed separately from the calculated amplitudes.*

Two-body breakup observables: d+ ^{58}Ni → p+n+^{58}Ni

CDCC calculations for **d+ ^{58}Ni** at 80 MeV :

- Continuum states with $\ell = 0, 2$.
- Proton and neutron intrinsic spins ignored.
- p/n+ ^{58}Ni from global optical potential.
- p+n simple Gaussian interaction describing deuteron g.s.

p + *n* c.m. angular distribution

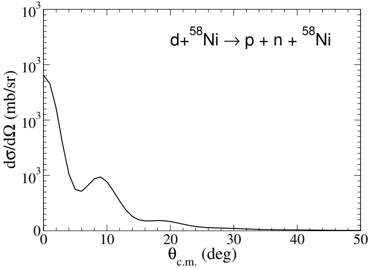

Excitation energy distribution

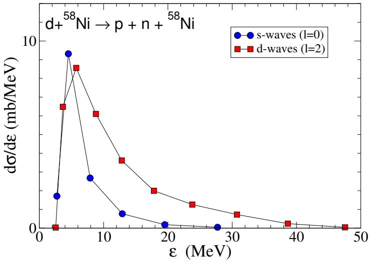

Breakup observables with CDCC: exclusive breakup of d+ ^{12}C → p+n+^{12}C

CDCC calculations for **d+ ^{12}C** at 56 MeV:

- Continuum states with $\ell \leq 8$ and ε_{max}=46 MeV.
- Proton and neutron intrinsic spins ignored
- p/n+ ^{58}Ni from Watson global optical potential
- p+n simple Gaussian interaction describing deuteron g.s.

Data: Matsuoka *et al.*, NPA391, 357 (1986).

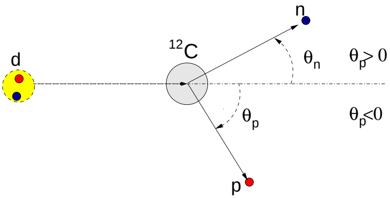

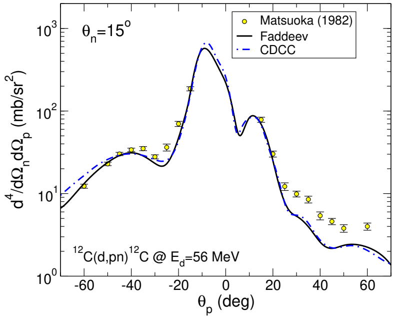

A.Deltuva, A.M.M., E.Cravo, F.M.Nunes, A.C.Fonseca, PRC 76, 064602 (2007)

Application of the CDCC method to other weakly bound two-body nuclei

The CDCC has been also applied to nuclei with a cluster structure:

- ^{6}Li=α + d ($S_{\alpha,d}$=1.47 MeV)
- ^{11}Be=^{10}Be + n (S_n=0.504 MeV)

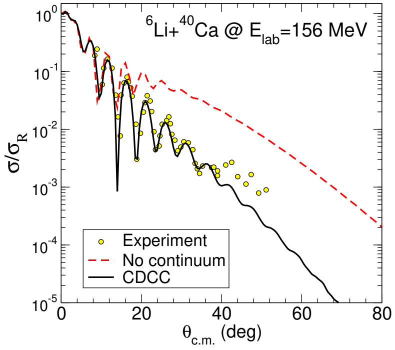

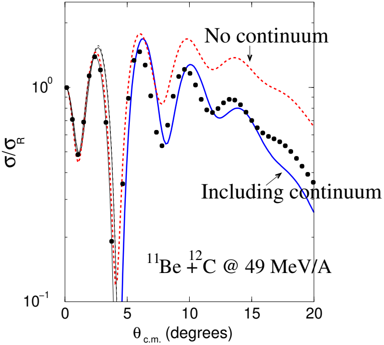

Exploring the continuum with breakup reactions

Electric response of weakly-bound nuclei

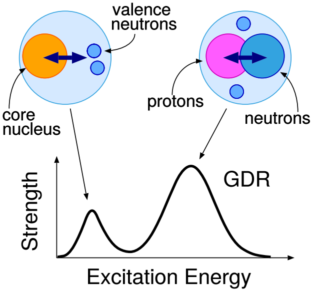

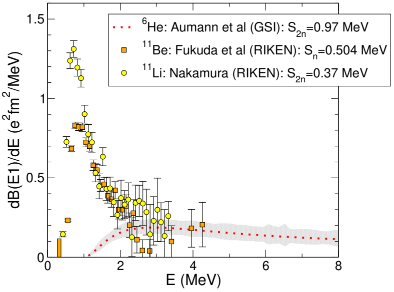

- The $E\lambda$ response can be quantified through the $B(E\lambda)$ probability:

$$\boxed{B(E\lambda; i \to f) = \frac{1}{2I_i + 1} |\langle \Psi_f \| \mathcal{M}(E\lambda) \| \Psi_i \rangle|^2}$$

- Neutron-halo nuclei have large $B(E1)$ strengths near threshold

How to probe/extract the $B(E1)$ of halo nuclei?

Example: ^{11}Be+^{208}Pb → ^{10}Be+ n+ ^{208}Pb measured at RIKEN (69 MeV/u).
Fukuda et al, PRC70, 054606 (2004))

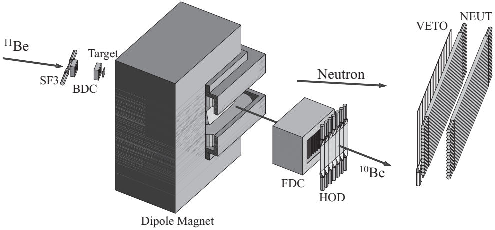

☞ ^{11}Be excitation energy can be reconstructed from core-neutron coincidences (*invariant mass method*)

What observables are measured in Coulomb dissociation experiments?

- In a fully exclusive experiment, one can in principle measure the angular and relative energy distribution of the ^{11}Be* system:

$$\boxed{\frac{d^2\sigma}{d\Omega\, dE_{\rm rel}}}$$

- Integrating over the angle or energy, single differential cross sections are obtained:

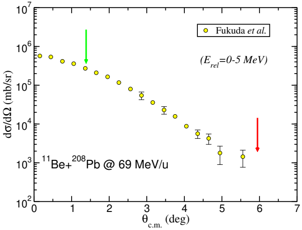

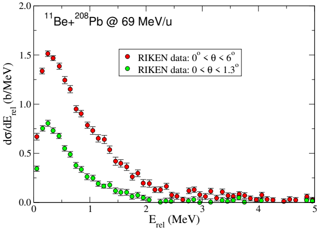

- In the Coulomb dominated region (i.e. small angles), the breakup cross section is expected to be dominated by the $dB(E\lambda)/dE$ distribution, but we need a theory that relates both observables.

Semiclassical 1st order Eλ excitation (Alder & Winther) (akin EPM method)

- For Eλ excitation to bound states ($0 \to n$):

$$\boxed{\left(\frac{d\sigma}{d\Omega}\right)_{0\to n} = \left(\frac{Z_t e^2}{\hbar v}\right)^2 \frac{B(E\lambda, 0 \to n)}{e^2 a_0^{2\lambda-2}} f_\lambda(\theta,\xi)} \qquad \xi_{0\to n} = \frac{(E_n - E_0)}{\hbar}\frac{a_0}{v}$$

- For continuum states (breakup):

$$\boxed{\frac{d\sigma(E\lambda)}{d\Omega dE} = \left(\frac{Z_t e^2}{\hbar v}\right)^2 \frac{1}{e^2 a_0^{2\lambda-2}} \frac{dB(E\lambda)}{dE} \frac{df_\lambda(\theta,\xi)}{d\Omega}}$$

- $dB(E\lambda)/dE$ can be extracted from small-angle Coulomb dissociation data.

$$\boxed{\frac{d\sigma}{dE}(\theta < \theta_{\max}) = \int_0^{\theta_{\max}} \frac{d\sigma(E\lambda)}{d\Omega dE} d\Omega \propto \frac{dB(E\lambda)}{dE}}$$

Extracting $B(E1)$ of ^{11}Be from ^{11}Be+^{208}Pb Coulomb dissociation

Common assumptions:

- Breakup dominated by Coulomb excitation
- Nuclear excitation, if present, can be estimated and added incoherently
- If the assumptions above are fulfilled, the extracted $dB(E\lambda)dE$ should be independent of the incident energy and target employed, since it reflects a structure property of the projectile.

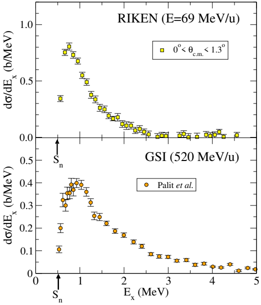

$$\frac{dB(E\lambda)}{dE} \propto \frac{d\sigma}{dE}$$

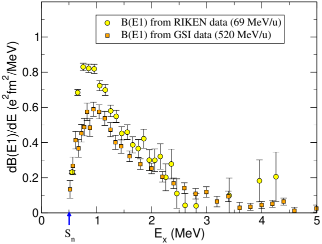

RIKEN: Fukuda et al, PRC70 (2004) 054606
GSI: Palit et al, PRC68 (2003) 034318

☞ *The extracted $dB(E\lambda)/dE$ distributions are reasonably compatible, but with apparent differences at the peak*

CDCC analysis of Coulomb dissociation data

- ➩ Nuclear excitation not negligible, even for small θ
- ➩ Nuclear contribution interferes with Coulomb
- ➩ Higher-order couplings can affect the cross sections
- ☞ These ingredients can be naturally incorporated within the CDCC method (at the expense of more complexity!)

E.g.: CDCC analysis based on two-body ^{10}Be+n model:

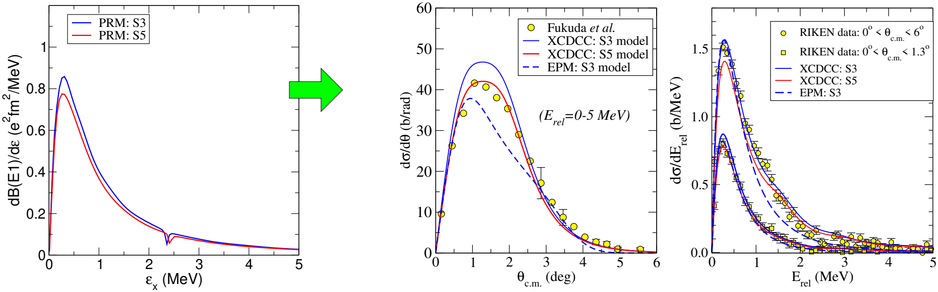

PLB 811 (2020) 135959

- ☞ Different structure models yield different $B(E1)$ strengths and hence different breakup cross sections
- ☞ Comparison with the angular distribution evidences the deficiencies of the semiclassical EPM model

Application to radiative capture reactions

Radiative capture: $b + c \rightarrow a + \gamma$

Photodissociation: $a + \gamma \rightarrow b + c$

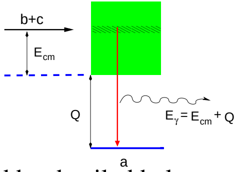

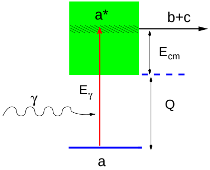

➯ Related by detailed balance:

$$\boxed{\sigma^{(rc)}_{E\lambda} = \frac{2(2J_a+1)}{(2J_b+1)(2J_c+1)} \frac{k_\gamma^2}{k^2} \sigma^{(phot)}_{E\lambda}} \qquad (\hbar k_\gamma = E_\gamma / c)$$

➯ Astrophysical S-factor:

$$\boxed{S(E_{\rm c.m.}) = E_{\rm c.m.} \sigma^{(rc)}_{E\lambda} \exp[2\pi\eta(E_{\rm c.m.})]}$$

➯ Capture cross sections are difficult to measure because they are very small at relevant astrophysical energies.

Direct determination of radiative capture cross sections

Example: $p+{}^{16}O \rightarrow {}^{17}F + \gamma$ Morlock, PRL79, 3837 (1997)

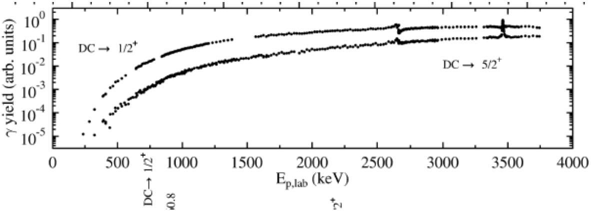

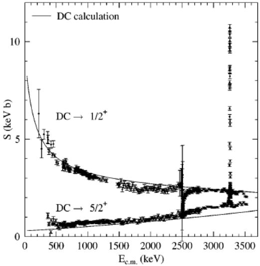

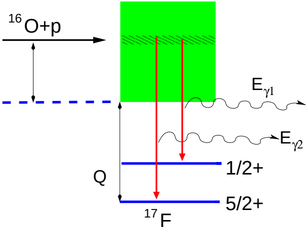

Indirect determination of radiative capture from Coulomb breakup

⇨ The photodissociation ($\gamma + a \to b + c$) cross section is related to the $B(E\lambda)$

$$\sigma^{\rm photo}_{E\lambda} = \frac{(2\pi)^3(\lambda+1)}{\lambda[(2\lambda+1)!!]^2}\left(\frac{E_\gamma}{\hbar c}\right)^{2\lambda-1}\frac{dB(E\lambda)}{dE}$$

⇨ Then, in 1st order semiclassical limit, the Coulomb breakup x-section is proportional to photodissociation x-section:

$$\boxed{\frac{d\sigma(E\lambda)}{d\Omega dE_\gamma} = \frac{1}{E_\gamma}\frac{dn_{E\lambda}}{d\Omega}\sigma^{\rm photo}_{E\lambda}}$$ (Equivalent Photon Method)

with the virtual photon number

$$\frac{dn_{E\lambda}}{d\Omega} = Z_t^2\alpha\frac{\lambda[(2\lambda+1)!!]^2}{(2\pi)^3(\lambda+1)}\xi^{2(1-\lambda)}\left(\frac{c}{v}\right)^{2\lambda}\frac{df_{E\lambda}}{d\Omega}$$

Radiative capture from Coulomb dissociation experiments

- Capture reactions have typically small cross sections
- As an alternative, one can indirectly obtain the capture cross sections from Coulomb dissociation experiments involving the same two-body projectiel:

$$\frac{d\sigma}{d\Omega dE_{c.m.}} \rightarrow \sigma^{(\mathrm{phot})}_{E\lambda} \rightarrow \sigma^{(rc)}_{E\lambda} \rightarrow S(E_{\mathrm{c.m.}})$$

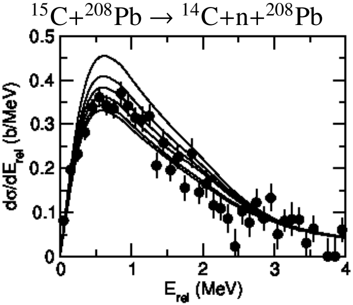

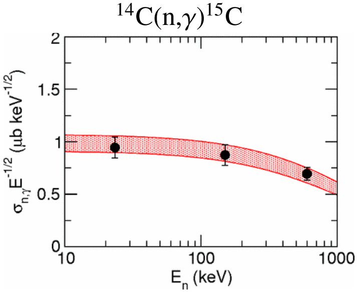

(dots: direct; shaded region: from Coulomb breakup)
Summers and Nunes, PRC 78, 011601(R), 2008

Exploring structures in the continuum

The continuum spectrum is not “homogeneous”; it contains in general energy regions with special structures, such as resonances and virtual states

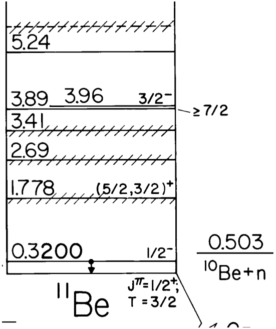

What is a resonance?

- It is a pole of the S-matrix in the complex energy plane.
- It is a structure on the continuum which may, or may not, produce a maximum in the cross section, depending on the reaction mechanism and the phase space available.
- The resonance occurs in the range of energies for which the phase shift is close to $\pi/2$.
- In this range of energies, the continuum wavefunctions is largely localized within the radial range of the potential.
- The continuum wavefunctions are not square normalizable. For practical reasons, a normalized wave-packet (or "bin") can be constructed to represent the resonance.

Distinctive features of a resonance

In the energy range of the resonance, the continuum wavefunctions have a large probability of being within the range of the potential.

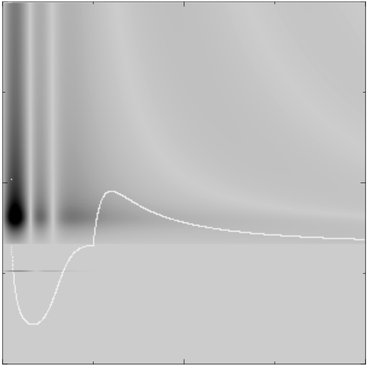

(Courtesy of C. Dasso)

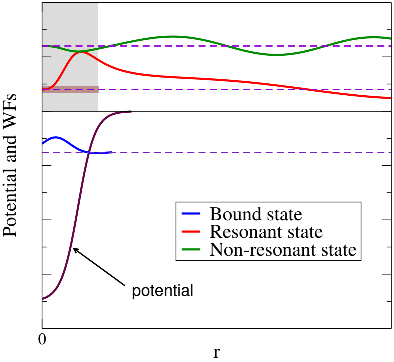

Resonances and phase-shifts

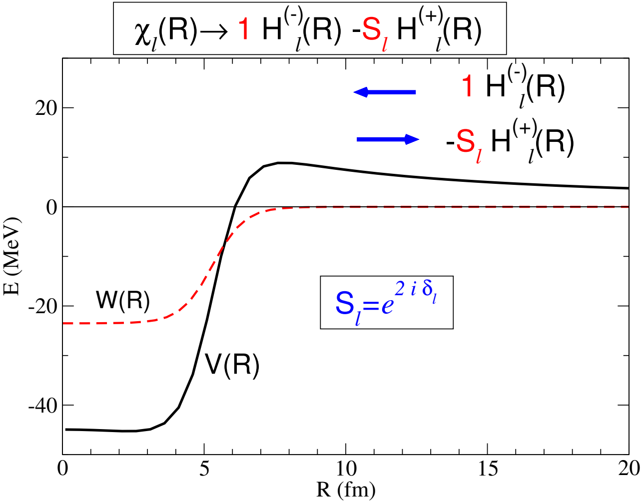

Resonances and phase-shifts

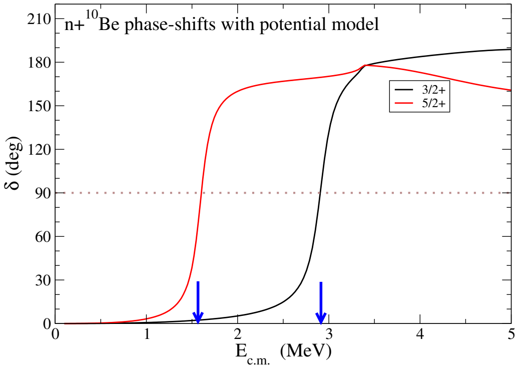

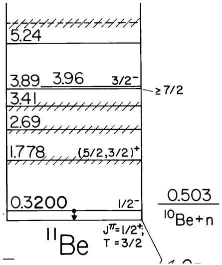

Resonances in nuclear breakup experiments

RIKEN data

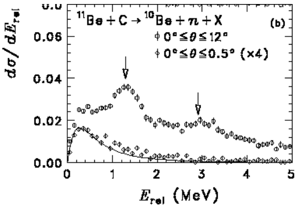

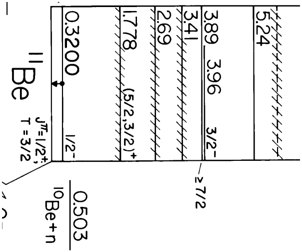

Fukuda *et al*, PRC70 (2004) 054606)

CDCC analysis

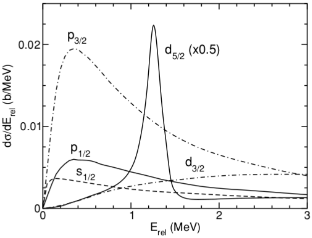

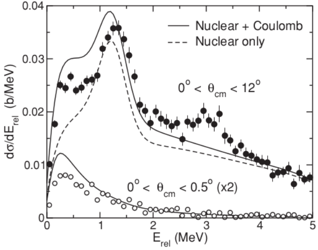

Howell *et al.*, JPG31 (2005) S1881

Suggested exercise

Consider a simple two-body model for a one-neutron halo nucleus. For E1 transitions, the electric transition probability is given by

$$\frac{dB(E1)}{dE_c} = \left(\frac{4\pi}{k}\right)^2 \frac{\mu k}{(2\pi)^3\hbar^2} \frac{3}{4\pi} \left(\frac{Ze}{A}\right)^2 \left|\langle \ell_i 010|\ell_f 0\rangle \int dr\, r^2 \phi_f(k,r)\phi_i(r)\right|^2$$

where μ is the reduced mass o the two-body system, $\phi_i(r)$ is the radial part of the ground-state wavefunction and $\phi_f(k,r)$ is the radial part of the positive-energy state with energy $E_c = \hbar^2 k^2/2\mu$ and asymptotic behaviour $\phi_f(k,r) \xrightarrow{r\gg} (kr) j_\ell(kr)$

- Show that, in the special case in which the final states are approximated by plane-waves, the $B(E1)$ distribution is related to the Fourier transform of the ground state wavefunction. Give arguments to justify that, in the case of weakly bound systems, the $B(E1)$ distribution is concentrated at low excitation energies.

Exercises

- In the situation above, the ground state wavefunction can be approximated by its asymptotic form which, for a s-wave configuration, can be written as

$$\phi_i(r) \simeq \sqrt{2k_0}e^{-k_0 r}/r.$$

Give the expression for k_0 in terms of the neutron separation energy (S_n) and the reduced mass of the neutron-core system. Compute it numerically for the ^{11}Be (^{10}Be+n) case.

- Show that, under these approximations, the $B(E1)$ distribution is given by

$$\frac{dB(E1)}{dE_c} = \frac{3\hbar^2}{\pi^2\mu}\left(\frac{Ze}{A}\right)^2 \frac{\sqrt{S_n}E_c^{3/2}}{(E_c+S_n)^4}.$$

Hint: $\int_0^\infty dr\, r^2 j_1(br)e^{-ar} = 2b/(a^2+b^2)^2$

- Show that the maximum of this $B(E1)$ distribution is located at $E_c = \frac{3}{5}S_n$.

Advanced CDCC applications

Extension to 3-body projectiles

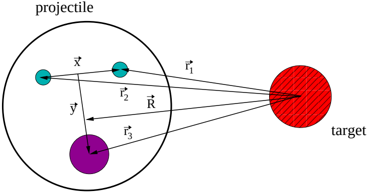

To extend the CDCC formalism, one needs to evaluate the new coupling potentials:

$$\boxed{V_{n;n'}(\mathbf{R}) = \int d\mathbf{r}\, \phi_n^*(\mathbf{x},\mathbf{y})\left\{V_{nt}(\mathbf{r}_1) + V_{nt}(\mathbf{r}_2) + V_{\alpha t}(\mathbf{r}_3)\right\}\phi_{n'}(\mathbf{x},\mathbf{y})}$$

☞ $\phi_n(\mathbf{x},\mathbf{y})$ three-body WFs for bound and continuum states: hyperspherical coordinates, Faddeev, etc (difficult to calculate!)

Calculation of three-body states in the HH formalism

$$\Psi^{j\mu}(\rho,\Omega) = \rho^{-5/2}\sum_{\beta} \chi^{j}_{\beta}(\rho)\mathcal{Y}^{j\mu}_{\beta}(\Omega) \qquad \beta \equiv \{K, l_x, l_y, l, S_x, J; I\}$$

Hyperspherical Harmonics (HH) expansion

hypermomentum $\widehat{K}$

$$\mathcal{Y}^{j\mu}_{\beta}(\Omega) = \left[\left(\Upsilon^{l_x l_y}_{K l m_l}(\Omega) \otimes \kappa_{S_x}\right)_J \otimes \phi_I\right]_{j\mu}$$

$$\Upsilon^{l_x l_y}_{K l m_l}(\Omega) = \varphi^{l_x l_y}_{K}(\alpha)\left[Y_{l_x}(\widehat{x}) \otimes Y_{l_y}(\widehat{y})\right]_{l m_l}$$

$$\varphi^{l_x l_y}_{K}(\alpha) = N^{l_x l_y}_{K}\,(\sin\alpha)^{l_x}\,(\cos\alpha)^{l_y}\,P_n^{l_x+\frac{1}{2},l_y+\frac{1}{2}}\,(\cos 2\alpha)$$

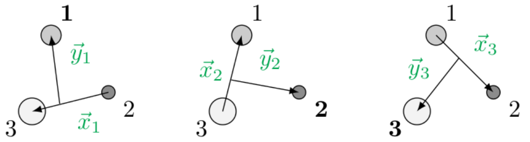

Jacobi coordinates $\{x, y, \widehat{x}, \widehat{y}\}$

Hyperspherical coordinates $\{\rho, \alpha, \widehat{x}, \widehat{y}\}$ $\qquad \rho = \sqrt{x^2+y^2} \qquad \alpha = \arctan\frac{x}{y}$

Calculation of three-body states in the HH formalism

$$\Psi^{j\mu}(\rho,\Omega) = \rho^{-5/2}\sum_{\beta} \chi^{j}_{\beta}(\rho)\mathcal{Y}^{j\mu}_{\beta}(\Omega) \qquad \beta \equiv \{K, l_x, l_y, l, S_x, J; I\}$$

Hyperspherical Harmonics (HH) expansion — hypermomentum $\widehat{K}$

$$\mathcal{Y}^{j\mu}_{\beta}(\Omega) = \left[\left(\Upsilon^{l_x l_y}_{K l m_l}(\Omega)\otimes\kappa_{S_x}\right)_J \otimes \phi_I\right]_{j\mu}$$

$$\Upsilon^{l_x l_y}_{K l m_l}(\Omega) = \varphi^{l_x l_y}_{K}(\alpha)\left[Y_{l_x}(\widehat{x})\otimes Y_{l_y}(\widehat{y})\right]_{l m_l}$$

$$\varphi^{l_x l_y}_{K}(\alpha) = N^{l_x l_y}_{K}(\sin\alpha)^{l_x}(\cos\alpha)^{l_y} P_n^{l_x+\frac{1}{2},l_y+\frac{1}{2}}(\cos 2\alpha)$$

Hyperradial functions are the solution of the coupled equations:

$$\left[-\frac{\hbar^2}{2m}\left(\frac{d^2}{d\rho^2} - \frac{15/4 + K(K+4)}{\rho^2}\right) - \varepsilon\right]\chi^{j}_{\beta}(\rho) + \sum_{\beta'} V^{j\mu}_{\beta'\beta}(\rho)\chi^{j}_{\beta'}(\rho) = 0$$

with coupling potentials $V^{j\mu}_{\beta'\beta}(\rho)$. Model space defined by **a given K_{max}**

Calculation of three-body states in the HH formalism

$$V^{j\mu}_{\beta'\beta}(\rho) = \left\langle \mathcal{Y}^{j\mu}_{\beta}(\Omega) \middle| V_{12} + V_{13} + V_{23} \middle| \mathcal{Y}^{j\mu}_{\beta'}(\Omega) \right\rangle + \delta_{\beta\beta'} V_{3\mathrm{b}}(\rho)$$

- V_{ij} interaction between pairs
  central, spin-orbit, spin-spin, tensor. To reproduce binary subsystem
- $V_{3\mathrm{b}}$ phenomenological three-body force
  diagonal term. Fixed to fine-tune the three-body energies

Pseudo-State (PS) method

$$\chi^{j}_{\beta}(\rho) = \sum_{i=0}^{N} C^{j}_{i\beta} U_{i\beta}(\rho)$$

expanded in $\mathcal{L}^2$ basis

N: number of hyperradial excitations included

$$\mathcal{H}\Psi^{j\mu}_{n} = \varepsilon_n \Psi^{j\mu}_{n}$$

- $\varepsilon_n < 0$ **bound states**
- $\varepsilon_n > 0$ **discretized continuum**

Calculation of three-body states in the HH formalism

Analytical **T**ransformed **H**armonic **O**scillator **(THO)** basis

$$U^{\text{THO}}_{i\beta}(\rho) = \sqrt{\frac{ds}{d\rho}} U^{\text{HO}}_{iK}[s(\rho)]$$

$$s(\rho) = \frac{1}{\sqrt{2}b} \left[\frac{1}{\left(\frac{1}{\rho}\right)^4 + \left(\frac{1}{\gamma\sqrt{\rho}}\right)^4} \right]^{\frac{1}{4}}$$

Example:

$\Psi^{j\mu}_n(\rho,\Omega)$ PS spectra, ε_n

$b = 0.7$ fm

The ratio γ/b controls the density of PS as a function of the energy.

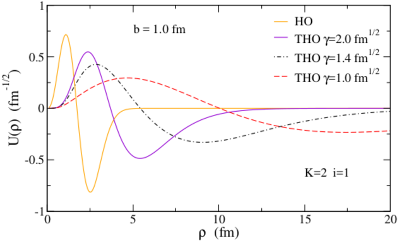

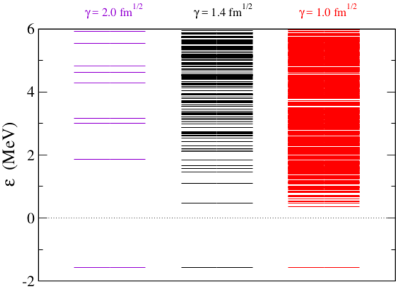

[PRC**88**(2013)014327]

Four-body CDCC calculations for ^{6}He scattering

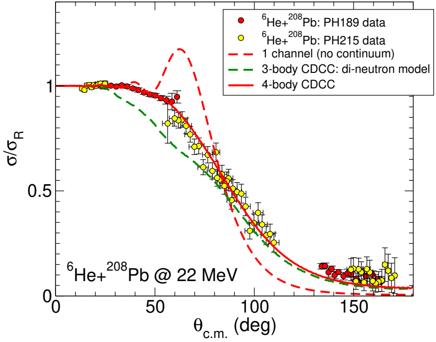

N.b.: 1-channel potential considers only g.s. → g.s. coupling potential:

$$\boxed{V_{00}(\mathbf{R}) = \int d\mathbf{r}\, \phi^*_{\text{g.s.}}(\mathbf{x},\mathbf{y}) \left\{V_{nt}(\mathbf{r}_1) + V_{nt}(\mathbf{r}_2) + V_{ct}(\mathbf{r}_3)\right\} \phi_{\text{g.s.}}(\mathbf{x},\mathbf{y})}$$

Data (LLN): Sánchez-Benítez et al, NPA 803, 30 (2008) L. Acosta et al, PRC 84, 044604 (2011)
Calculations: Rodríguez-Gallardo et al, PRC 80, 051601 (2009)

Polarization potential from CDCC calculations

$$\left[E-\varepsilon_0-\hat{T}_{\mathbf{R}}-V_{0,0}(\mathbf{R})\right]\chi_0(\mathbf{R})=\sum_{i\neq 0}V_{i,0}(\mathbf{R})\chi_i(\mathbf{R})\equiv U_{\mathrm{TELP}}(R)\chi_0(\mathbf{R}).$$

Example: ^{6}He+^{208}Pb at 22 MeV

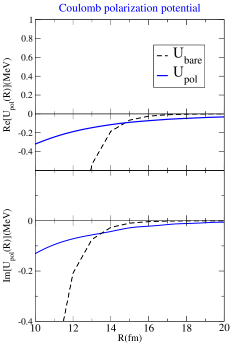

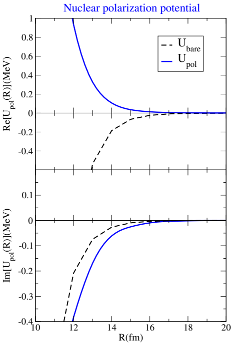

- Polarization potentials are long-ranged.
- Both nuclear and Coulomb couplings contribute to the polarization effect.

Beyond the strict few-body picture: the effect of core excitation

To what extent can one ignore the dynamics of the core?

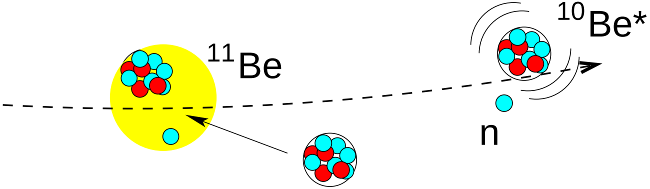

Few-body versus Microscopic

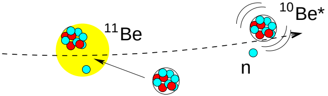

Microscopic models

- ✔ Fragments described microscopically
- ✔ Realistic NN interactions (Pauli properly accounted for)
- ✖ Numerically demanding / not simple interpretation.

Few-body versus Microscopic

Microscopic models

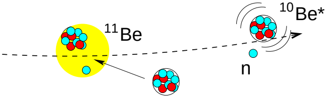

- ✔ Fragments described microscopically
- ✔ Realistic NN interactions (Pauli properly accounted for)
- ✖ Numerically demanding / not simple interpretation.

Inert cluster models

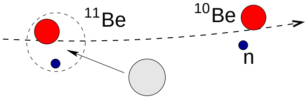

- ✖ Ignores cluster excitations (only few-body d.o.f).
- ✖ Phenomenological inter-cluster interactions (aprox. Pauli).
- ✔ Exactly solvable (in some cases).
- ✔ Achieved for 3-body and 4-body (eg. coupled-channels, Faddeev).

Few-body versus Microscopic

Microscopic models

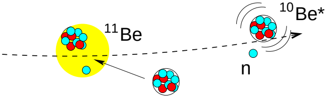

- ✔ Fragments described microscopically
- ✔ Realistic NN interactions (Pauli properly accounted for)
- ✖ Numerically demanding / not simple interpretation.

Non-inert-core few-body models

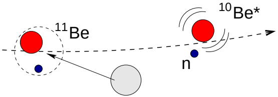

- ✔ Few-body + some relevant collective d.o.f.
- ✔ Pauli approximately accounted for.
- ✔ Achieved for 3-body problems (coupled-channels, Faddeev).

Inert cluster models

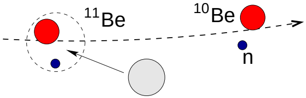

- ✖ Ignores cluster excitations (only few-body d.o.f).
- ✖ Phenomenological inter-cluster interactions (aprox. Pauli).
- ✔ Exactly solvable (in some cases).
- ✔ Achieved for 3-body and 4-body (eg. coupled-channels, Faddeev).

Effect of core excitation in scattering observables

- Elastic scattering (adiabatic recoil model): K. Horii *et al*, PRC81 (2010) 061602
  - *Some effects found in* ^{8}B +^{12} C.
- Transfer (DWBA, CCBA, Faddeev): Winfield *et al*, NPA 683 (2001) 48, Fortier *et al*, PLB 461 (1999) 22, Deltuva, Phys.Rev. C 88, 011601 (2013)
- Knock-out: Batham et al, PRC71, 064608 (2005)
  - Small effect on stripping; large effect on diffraction
- Breakup
  - DWBA: Crespo *et al*, PRC83, 044622 (2011), A.M.M. *et al* PRC85, 054613 (2012), A.M.M. and J.A. Lay, PRL109, 232502 (2012)
  - CDCC: Summers *et al*, PRC74, 014606(2006), PRC76,014611 (2007), De Diego *al*, PRC89, 064609 (2014), PRC 95, 044611 (2017)

How do core excitations affect the breakup of weakly-bound nuclei?

Core excitations will affect:

1. the structure of the projectile ⇨ core-excited admixtures

$$\boxed{\Psi_{JM}(\vec{r},\xi) = \sum_{\ell,j,I} \left[\varphi^{J}_{\ell,j,I}(\vec{r}) \otimes \Phi_I(\xi)\right]_{JM}}$$

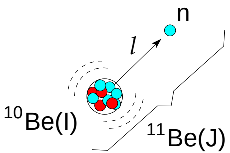

2. the dynamics ⇨ collective excitations of the ^{10}Be during the collision compete with halo (single-particle) excitations.

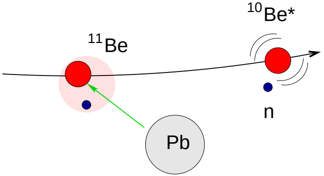

⇨ Both effects have been recently implemented in an extended version of of the CDCC formalism (CDCC): Summers *et al*, PRC74 (2006) 014606, R. de Diego *et al*, PRC 89, 064609 (2014)

Core excitation in reactions: *frozen-halo* picture

$$\boxed{\Psi_{JM}(\vec{r},\xi) = \left[\varphi^{J}_{\ell,j}(\vec{r}) \otimes \Phi_I(\xi)\right]_{JM}}$$

- $\varphi^{J}_{\ell,j}(\vec{r})$= valence particle wavefunction
- $\Phi_I(\xi)$= core wavefunction (*frozen*)

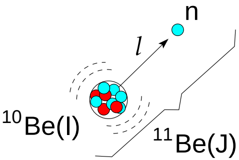

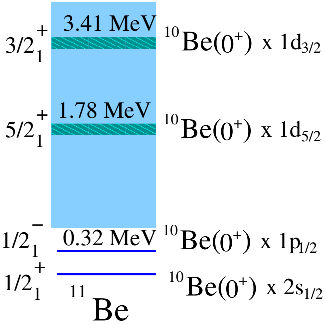

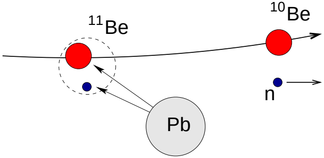

Core excitation in reactions: *frozen-halo* picture

$$\boxed{\Psi_{JM}(\vec{r},\xi) = \left[\varphi^J_{\ell,j}(\vec{r}) \otimes \Phi_I(\xi)\right]_{JM}}$$

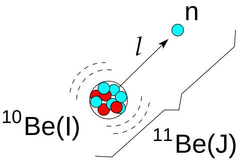

- $\varphi^J_{\ell,j}(\vec{r})$= valence particle wavefunction
- $\Phi_I(\xi)$= core wavefunction (*frozen*)

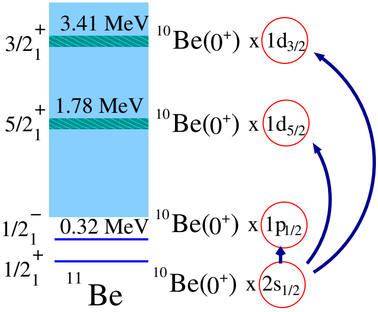

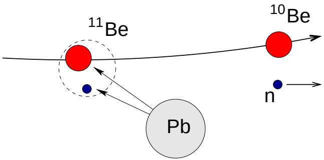

Core excitation mechanism in breakup

$$\Psi_{JM}(\vec{r},\xi) = \sum_{\ell,j,I} \left[\varphi^{J}_{\ell,j,I}(\vec{r}) \otimes \Phi_I(\xi)\right]_{JM}$$

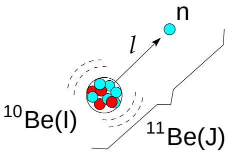

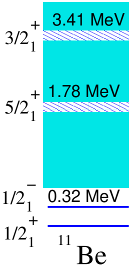

$e[\,^{10}\mathrm{Be}(0^+) \times 1d_{3/2}\,] + f\,[\,^{10}\mathrm{Be}(2^+) \times 2s_{1/2}\,]$

$c[\,^{10}\mathrm{Be}(0^+) \times 1d_{5/2}\,] + d\,[\,^{10}\mathrm{Be}(2^+) \times 1d_{5/2}\,]$

$A[\,^{10}\mathrm{Be}(0^+) \times 1p_{1/2}\,] + B\,[\,^{10}\mathrm{Be}(2^+) \times 1p_{3/2}\,]$

$a[\,^{10}\mathrm{Be}(0^+) \times 2s_{1/2}\,] + b\,[\,^{10}\mathrm{Be}(2^+) \times 1d_{5/2}\,]$

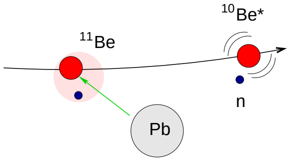

Core excitation mechanism in breakup

$$\Psi_{JM}(\vec{r},\xi) = \sum_{\ell,j,I} \left[\varphi^{J}_{\ell,j,I}(\vec{r}) \otimes \Phi_I(\xi)\right]_{JM}$$

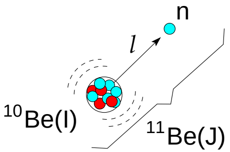

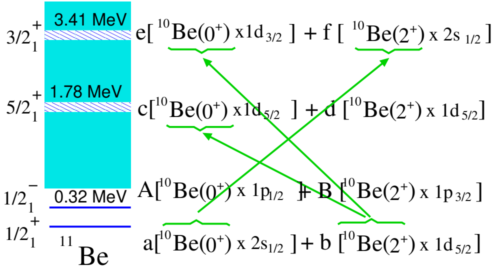

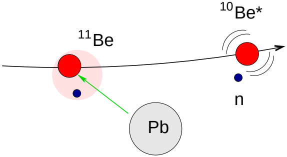

☞ *Dynamic core excitation contributes to the inelastic/breakup probabilities*

Extending CDCC to include core excitations

- Standard CDCC $\Rightarrow$ use coupling potentials:

$$\boxed{V_{\alpha;\alpha'}(\mathbf{R}) = \langle \Psi^{\alpha'}_{J'M'}(\vec{r}) | V_{vt}(r_{vt}) + V_{ct}(r_{ct}) | \Psi^{\alpha}_{JM}(\vec{r}) \rangle}$$

- Extended CDCC (XCDCC) $\Rightarrow$ use generalized coupling potentials

$$\boxed{V_{\alpha;\alpha'}(\mathbf{R}) = \langle \Psi^{\alpha'}_{J'M'}(\vec{r}, \xi) | V_{vt}(r_{vt}) + V_{ct}(r_{ct}, \xi) | \Psi^{\alpha}_{JM}(\vec{r}, \xi) \rangle}$$

  - $\Psi^{\alpha}_{JM}(\vec{r}, \xi)$: projectile WFs involving core-excited admixtures (structure).
  - $V_{ct}(r_{ct}, \xi)$: non-central potential allowing for core excitations/de-excitations (dynamic core excitation).

- Summers *et al*, PRC74 (2006) 014606 (bins)
- R. de Diego *et al*, PRC 89, 064609 (2014) (THO pseudo-states)

Evidences of core excitation in nuclear breakup

Structure part: particle-core model

- Particle-plus-core Hamiltonian:

$$H_{\rm proj} = T_r + h_{\rm core}(\xi) + V_{vc}(\vec{r}, \xi)$$

- Projectile states expanded in $|\alpha;\ JM\rangle \equiv |(\ell s)j, I; JM\rangle$ basis:

$$\boxed{\Psi_{JM}(\vec{r}, \xi) = \sum_{\ell,j,I} R^J_{\ell,j,I}(r) \left[[Y_\ell(\hat{r}) \otimes \chi_s]_j \otimes \Phi_I(\xi) \right]_{JM}}$$

- The unknowns $R^J_{\ell,j,I}(r)$ can be obtained by direct integration of the Schrödinger equation or by diagonalization in a suitable discrete basis (pseudo-state method).

Valence-core and core-target interactions in a simple collective model

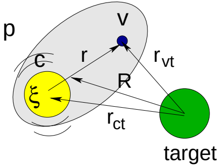

➩ Valence-core:

$$V_{vc}(\vec{r},\xi) \simeq V_{vc}^{(0)}(r) - \delta_2 \frac{dV_{vc}^{(0)}}{dr} Y_{20}(\hat{r})$$

➩ Core-target:

$$V_{ct}(\vec{r}_{ct},\xi) \simeq \underbrace{V_{ct}^{(0)}(r_{ct})}_{\text{Valence excitation}} \underbrace{- \delta_2 \frac{dV_{ct}^{(0)}}{dr} Y_{20}(\hat{r}_{ct})}_{\text{Core excitation}}$$

$\delta_2 = \beta_2 R_0$=deformation length

➩ *More sophisticated models for the projectile structure and core-target interaction are possible!*

Exclusive breakup measurements of halo nuclei

RIKEN experiments:

- ^{19}C+p: Satou et al., PLB660 (2008) 320
- ^{11}Be+^{12}C: Fukuda et al, PRC70, 054606 (2004)

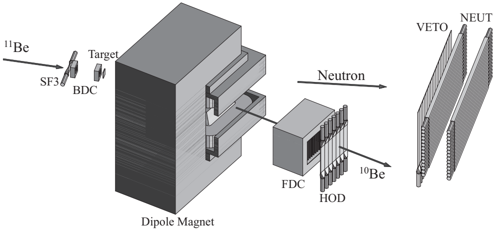

- Excitation energy and angular distribution of the projectile can be reconstructed from core-neutron coincidences (*invariant mass method*)

Application to ^{11}Be: spectroscopic factors

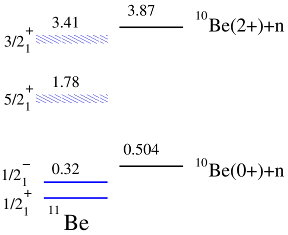

State	Model	$\|0^+ \otimes (\ell s)j\rangle$	$\|2^+ \otimes s_{1/2}\rangle$	$\|2^+ \otimes d_{5/2}\rangle$
$1/2^+$ (g.s.)	PRM	0.857	–	0.121
	SM (WBT)	0.76	–	0.184
$5/2^+$ (1.78 MeV)	PRM	0.702	0.177	0.112
	SM(WBT)	0.682	0.177	0.095
$3/2^+$ (3.41 MeV)	PRM	0.165	0.737	0.081
	SM(WBT)	0.068	0.534	0.167

- $1/2^+_1, 5/2^+_1 \Rightarrow$ dominant ^{10}Be(gs) $\otimes\, nlj$ configuration
- $3/2^+_1 \Rightarrow$ dominant ^{10}Be$(2^+) \otimes 2s_{1/2}$ configuration

Evidence of *dynamical* core excitations in p(^{11}Be,p') at 64 MeV/u (MSU)

Data: Shrivastava et al, PLB596 (2004) 54 (MSU)

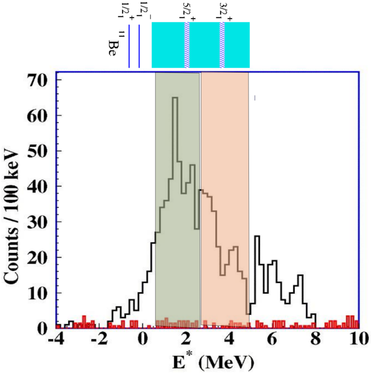

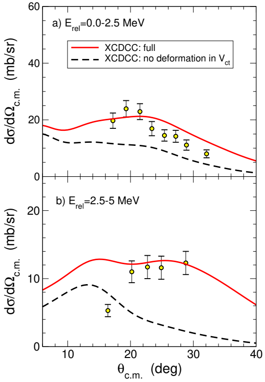

R.de Diego et al, PRC85, 054613 (2014)

- E_{rel}=0–2.5 MeV contains $5/2^+$ resonance (expected single-particle mechanism)
- E_{rel}=2.5–5 MeV contains $3/2^+$ resonance (expected core excitation mechanism)

⇨ Dynamical core excitations give additional (and significant!) contributions to breakup

Dominance of *dynamical* core excitations in ^{19}C resonant breakup

$^{19}C + p \rightarrow {}^{18}C + n + p$ @ 70 MeV/u (RIKEN)

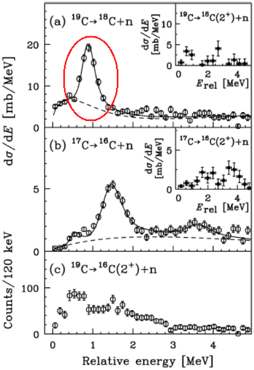

Satou et al, PLB660 (2008) 320

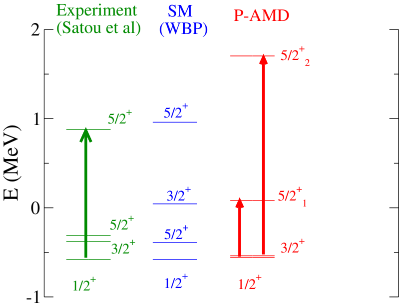

- No general consensus about the ^{19}C spectrum.
- Resonant peak consistent with $5/2^+_1$, $5/2^+_2$ or even a combination of both.

Dominance of *dynamical* core excitations in ^{19}C resonant breakup

^{19}C + p → ^{18}C+n + p @ 70 MeV/u (RIKEN)

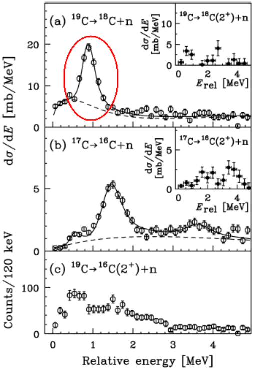

Satou et al, PLB660 (2008) 320

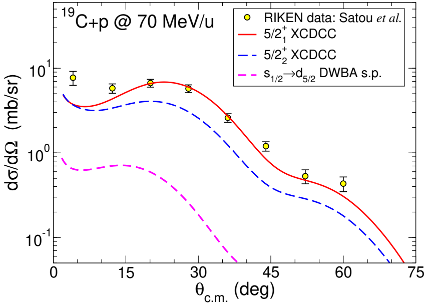

J.A. Lay et al, PRC 94, 021602 (2016)

⇨ The core-excitation mechanism gives the dominant contribution to the cross section